*Vladimir D. Jović**

Institute for Multidisciplinary Research University of Belgrade, Belgrade, Serbia

Review paper
ISSN 0351-9465, E-ISSN 2466-2585
https://doi.org/10.62638/ZasMat1744

Zastita Materijala 67 (2)
391 - 408 (2026)

Determination of adsorption capacitance and adsorption resistance in the process of anions adsorption

ABSTRACT

In this work, adsorption processes of different anions onto Ag singlecrystalsand polycrystals have been discussed and reviewed. Electrochemical Impedance Spectroscopy (EIS) and differential capacitance (C_{diff} vs. ω) measurements for all cases were presented. Fitting of experimental results was performed by using commercial software for fitting EIS results defined by Gamry Instruments Inc. (EIS 300), as well as by equation for C_{diff} vs. ω dependence.C_{diff} vs. ω dependence has been defined in several previous investigations for anion adsorption, containing Constant Phase Element (CPE_{dl}), corresponding to the double layer capacitance(C_{dl}), connected in parallel with the adsorption capacitance (C_{ad}) and adsorption resistance (R_{ad}). It was shown that significant difference in parameters for anion adsorption obtained by both fitting procedures could be explained by the fact that in the EIS fitting analysis (presented either as Nyquist, or Bode plot, or Z' vs. ω and Z'' vs. ω plots) two functions are fitted simultaneously, while in the case of C_{diff} vs. ω dependencesonly one function, containing all parameters of the equivalent circuit, is fitted. It should be emphasized that the explanation for the difference in fitting procedures is for the first time presented in this work.

Keywords:*Silver single crystals, anion adsorption mechanism, EIS, CPE, C_{diff} vs. ω dependence.*

1. INTRODUCTION

1.1. Differential capacitance measurements

Differential capacitance measurements (C_{diff} vs. E curves) were introduced in electrochemistry with the beginning of double layer structure investigations as a suitable technique for determining the C_{dl} on both, liquid (mercury) and solid metal electrodes [1,2]. This technique was very convenient for determining the potential of zero charge, E_{pzc} on solid electrodes as a minimum on C_{diff} vs. E curves [1-3]. Since the minimum existed only in the presence of a diffuse part of the double layer [4,5] these experiments were performed in dilute solutions of the concentrations lower than 10^{-2} M, usually of the order of 10^{-3} M [6,7]. In all these experiments solution resistance (R_s) had to be compensated in order to obtain the real value of C_{dl}. In such a case the value of C_{diff} was equal to the value of C_{dl} and was independent of frequency. Accordingly measurement at one frequency was sufficient to determine the value of the double layer capacitance.

With introduction of single crystal surfaces, this technique in combination with cyclic voltammetry (CV), has frequently been used for determining E_{pzc} as well as adsorption behavior of different anions. Typical frequencies for these measurements varied between 10 Hz and 20 Hz [7], while the sweep rate used was usually 5 - 10 mV s^{-1}. For interpretation of the obtained results concerning adsorption of anions it was assumed that the "specific adsorption" of anions does not involve the charge transfer between the electrode surface and adsorbed anions.

About 35 years ago the equivalent circuit composed of C_{dl} connected in parallel with R_{ct} and C_{ad} was used for the first time in the literature for the analysis of adsorption of acetate anions onto Ag(111)by V.D. Jović, B.M. Jović and R. Parsons [8]. By the analysis of proposed equivalent circuit it was shown that R_{ct} and C_{ad}could be obtained from the dependence $1/Y'_c$ vs. $1/\omega^2$ presented by equation

$$\frac{1}{Y_c'} = R_{ct} + \frac{1}{R_{ct}C_{ad}{}^2}\frac{1}{\omega^2} \qquad (1)$$

where Y'_c represents admittance corrected for the R_s (R_{ct}could be obtained from the intercept, while C_{ad}could be obtained from a slope of this

*Corresponding author: Vladimir D. Jović
E-mail:vladajovic@imsi.bg.ac.rs
Paper received: 18.01.2026.
Paper accepted: 25.02.2026.

dependence). Unfortunately it was discovered that straight line dependences could be obtained only in the selected frequency range of 10 Hz to 100 Hz.The same equivalent circuit, with adsorption resistance (R_{ad}) instead of R_{ct}, has later been used for the analysis of fluoride, acetate and sulfate anions onto Ag single crystals [9-11], as well as OH^- species adsorption onto Cu(111) from fluoride or sulfate containing solutions of different pH [12]. Later on, another component (Warburg impedance) has been added to the previously described equivalent circuit (in series with R_{ad} and C_{ad}) in order to explain adsorption of halide anions of low concentrations (0.1 – 1.0 mM) onto gold single crystal surfaces [13,14]. This approach wasn't new since identical equivalent circuit had been proposed by M. Sluytres-Rehbach et al. [15] about fifty five years ago. It was assumed that single crystal surface behaves as an ideal, homogeneous electrode surface, having no "fractal character", nor heterogeneous surface[13,14]. T. Pajkossy et al. [14] also reported almost ideal double layer behavior for Au(111) and Au(100) in dilute $HClO_4$ solution in the frequency range between 0.1 Hz and 5 kHz. They found that capacitance exhibits only minor frequency dependence at potentials more negative than 0.4 V , with the ratio of the capacitance measured at 1 Hz and at 0.1 kHz differing from unity by a few percent's only. They pointed out that the "frequency dispersion" could be a consequence of either phase transition at the interface, or specific adsorption of anions. In both papers [13,14] "frequency dispersion" observed in the presence of specific adsorption has been explained by the adsorption of anions controlled by their diffusion. All equivalent circuits considered fin these analysis are presented in Figure 1 (a) and (b).

Z. Kerner et al. [16] demonstrated that the frequency dependence of capacitance on solid electrodes was due to the atomic scale non-homogeneities rather than due to the geometry aspect of roughness. They criticized old physical theories used for explaining capacitance dispersion as a function of surface roughness [17-20] and pointed out physico-chemical approach of T. Pajkossy [21,22], claiming that the origin of the capacitance dispersion can be allocated in the double layer and that it can be attributed to the presence of atomic scale non-homogeneities – "disorder" of the electrode surface, together with the presence of some kinetic process, most probably specific adsorption of anions [16].

Although ordered structure $(\sqrt{3}\,x\,\sqrt{3})R30^o$ of adsorbed chloride onto Ag(111) had been detected by ex situ LEED and Auger spectroscopy techniques [23,24], introduction of in situ techniques (STM and surface X-ray scattering) in the investigation of the structure of adsorbed anions onto single crystal faces provided significant contribution to the understanding of this process [25-30]. It was shown that in the case of chloride and bromide anions adsorption onto Au single crystals incommensurate, hexagonal-close-packed monolayers, compressing uniformly with increasing potential were formed [26-28]. The ad-atom spacing of these compressed structures was found to approach van der Waals diameter, indicating at least partial discharge of anions [26-28]. Th. Wandlowski et al. [29] showed by chronocoulometry (thermodynamic analysis) and surface X-ray scattering (SXS) that in the case of bromide adsorption onto Ag(100) ordered c(2x2) structure has been formed, with the charge number being -0.85 ± 0.05 at constant chemical potential, indicating also existence of partial charge transfer between adsorbed anions and the substrate. It is interesting to note that the C_{diff} vs. E curve, obtained at a frequency of 18 Hz, 10 mV peak-to-peak amplitude and sweep rate of 10 mV s^{-1}, presented by these authors [29], was characterized by the hysteresis (Figure 1 of Ref. [29]) for bromide concentrations lower than 1.0mM. The authors concluded that such data were not adequate for determination of any thermodynamic quantities [29] primarily due to mass-transfer limitations. Identical conclusions concerning C_{diff}vs. Emeasurements at single frequency and electrosorption valence were made by Shi et al. [31] in the study of chloride anions adsorption onto Au(111) face. In situ X-ray absorption fine structure (XAFS) studies of bromide adsorption onto Ag(111) revealed the formation of AgBr(111) monolayer with the Br-Ag bond distance of 2.72 ± 0.05 Å, corresponding to the complete charge transfer between Br anions and Ag(111) surface [30]. Hence, one can conclude that structural in situ X-ray analysis [26-28,30] and even thermodynamic analysis [29] of anion adsorption, indicated the presence of partial charge transfer between anions and substrate during the process of anion adsorption.

2. THEORETICAL CONSIDERATION AND SIMULATION OF DIFFERENTIAL CAPACITANCE FOR DIFFERENT CASES OF ANION ADSORPTION

The dependences of C_{diff} vs. ω for different cases of anion adsorption processes for "ideal (homogeneous)" and "real surfaces" (introducing CPE_{dl} instead of C_{dl}) have been analyzed by calculation of C_{diff} vs. ω.Two cases are considered: 1) C_{dl}represented by a parallel plate condenser (assuming ideal, homogeneous surface) and 2) C_{dl}represented by a CPE_{dl} (assuming heterogeneous surface). C_{diff} vs. ω dependences were simulated in the frequency range from $\omega = 10^{-2}$ Hz to $\omega = 10^5$ Hz, since this is the most wide range of frequencies offered by the producers of EIS measurement systems. All considered equivalent circuits are presented in Figure 1.

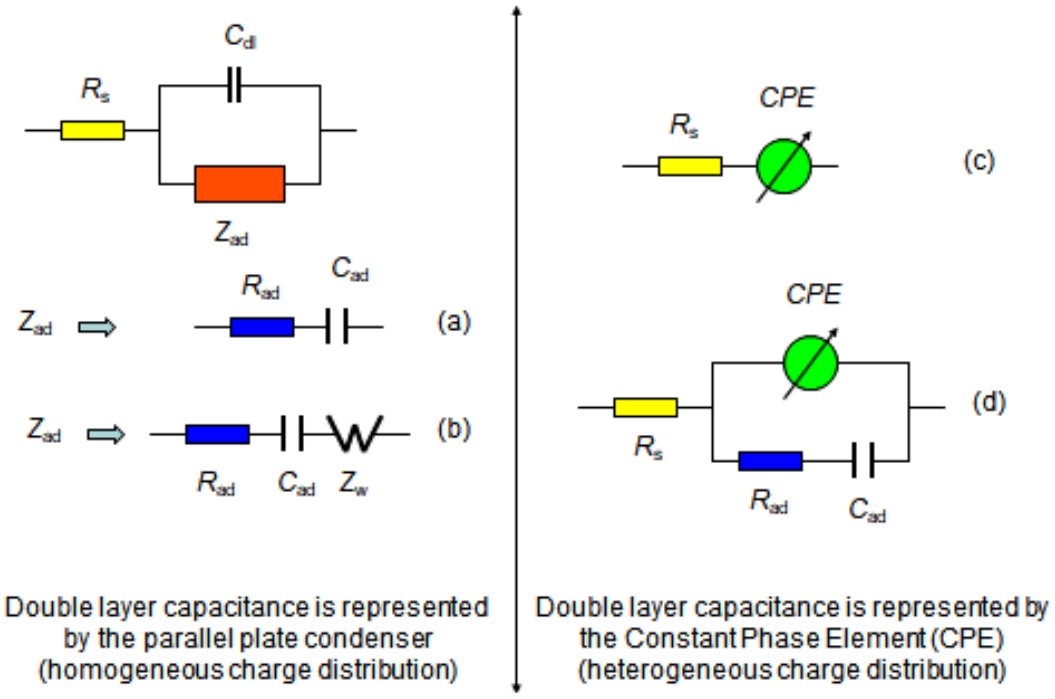

Figure 1. Equivalent circuits for anion adsorption on the "ideal surface" (left) and on the "real surface" (right)

2.1. Ideal, homogeneous surface

2.1.1. Ideal double layer behavior without adsorption and diffusion of anions

Equivalent circuit for ideal double layer behavior of the electrode impedance is presented by solution resistance $R_s$and double layer capacitance C_{dl} connected in series. Differential capacitance is by definition imaginary component of electrode admittance over frequency and for such equivalent circuit is given by the equation

$$C_{diff} = \frac{Y''}{\omega} = \frac{C_{dl}}{1+\omega^2 C_{dl}^2 R_s^2} \qquad (2)$$

In most cases $1 >> \omega^2 C_{dl}^2 R_\Omega^2$ and accordingly $C_{diff} \approx C_{dl}$. In dilute solutions with high value of R_s the value of C_{diff} could be influenced by the R_s[8-10]. Hence, imaginary component of electrode admittance should be corrected for $R_s$in order to obtain the real value of C_{dl}. This could be done either by compensating R_s during the differential capacitance measurements (using *IR* compensation technique on the potentiostat), or by subtracting it from the real component of electrode impedance, $Z'_{corr} = Z' - R_s$ and calculating Y''_{corr} by following equation (R_s - determined from the high frequency intercept of impedance diagrams, or by some other technique)

$$Y''_{corr} = \frac{Z''}{(Z'_{corr})^2 + (Z'')^2} \qquad (3)$$

Hence, using Y''_{corr} for determining C_{diff} ($Y''_{corr}/\omega = C_{diff}$) it is possible to obtain the real value of differential capacitance.

2.1.2. Ideal double layer behavior with specific adsorption of anions

In the presence of specific adsorption presented by the $R_{ad}$and C_{ad}connected in series (Figure 1 (a,b,d), C_{diff} (corrected for R_s) should depend on frequency [8-10,12]. The simplest case of specific adsorption is usually represented by the equivalent circuit shown in the Figure 1(a), with adsorption impedance (Z_{ad}) being composed ofR_{ad} and C_{ad} connected in series [8-10].

Simulated C_{diff} vs. ω dependences, obtained in the frequency range from $\omega = 10^{-2}$ Hz to $\omega = 10^5$ Hz for this equivalent circuit for different values of C_{ad} (80 μF, 140 μF and 220 μF, respectively)are presented in Figure 2(a).As seen in the figure the value of C_{dl} can be determined by using C_{diff} values recorded at frequencies higher than certain critical frequency ω_c(dl) (see Figure 2), which is independent on the values of C_{dl} and C_{ad}. In the frequency range from ~ 5 Hz to 1000 Hz, between ω_c(ad) andω_c(dl),C_{diff}depends on frequency and cannot be used for determining values of C_{dl} and C_{ad}. Hence, C_{diff} obtained at a single frequency in that particular region, does not represent neither pure C_{dl}, nor $C_{dl}+C_{ad}$. With the increase of the value of C_{ad} the sum of $C_{dl}+C_{ad}$ could be obtained only at frequencies lower thanω_c(ad). Of course, this is valid only for R_{ad}= 50 Ω used for this simulation. C_{diff} vs. ωfunction also depends on the value of R_{ad},

as shown in Figure 2(b).With increasing the value of R_{ad} critical frequency for accurate determination of $C_{ad}(\omega_c(ad))$ decreases and if the process of adsorption becomes very slow (high values of R_{ad}, R_{ad}> 5000 Ω),C_{ad} cannot be determined from the value of C_{diff} recorded at frequencies higher than ~0.1 Hz (this is valid for the values of C_{ad} and C_{dl}given in the figure). Hence, for faster adsorption processes C_{diff} represents the sum of C_{dl} + C_{ad} at frequencies lower than about 20 Hz. Critical frequency for C_{dl} determination, ω_c(dl), also increases with decreasing R_{ad}, being about 0.1 Hz for R_{ad} = 50000 Ω and about 10 Hz for R_{ad} = 50 Ω. It is important to note that in the "intermediate frequency range", between ω_c(ad) and ω_c(dl), measured values of C_{diff}do not represent the real value of either C_{dl} andC_{ad}, or their sum.

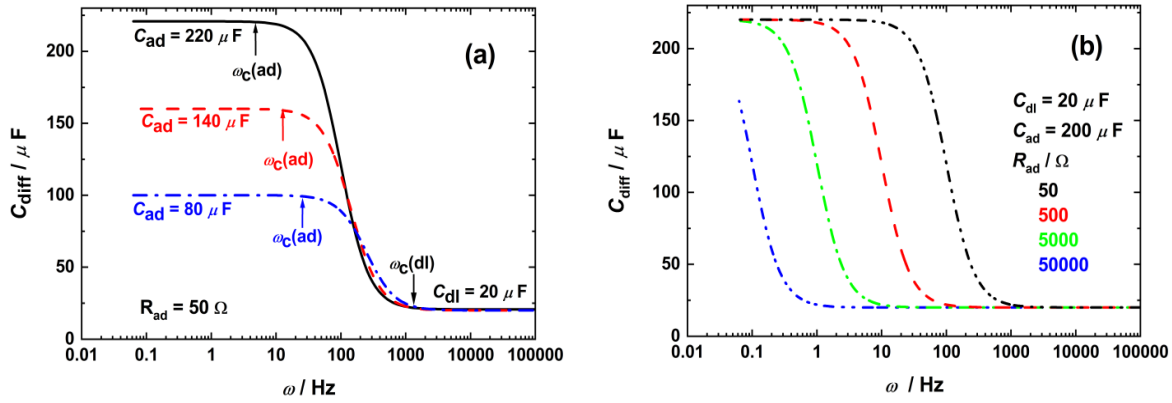

Figure 2. (a) The influence of C_{ad} on the shape of C_{diff} vs. ω dependences for equivalent circuit presented in Figure 1(a), (b) The influence of R_{ad} on the shape of C_{diff} vs. ω dependences for equivalent circuit presented in Figure 1(a)

2.1.3. Ideal double layer behavior with specific adsorption controlled by diffusion of anions

If the process of anion adsorption is controlled by the diffusion of anions to the electrode surface Warburg impedance must be added in series to R_{ad} and C_{ad} [13-15], as it is presented in Figure 1(b). Assuming that the diffusion coefficient for anions amounts to 1 x 10^{-5}cm^2 s^{-1} and using equation for Warburg constant σ [32] C_{diff} vs. ω curves are simulated for different concentrations of anions (0.01 mM to 10 mM), Figure 3.

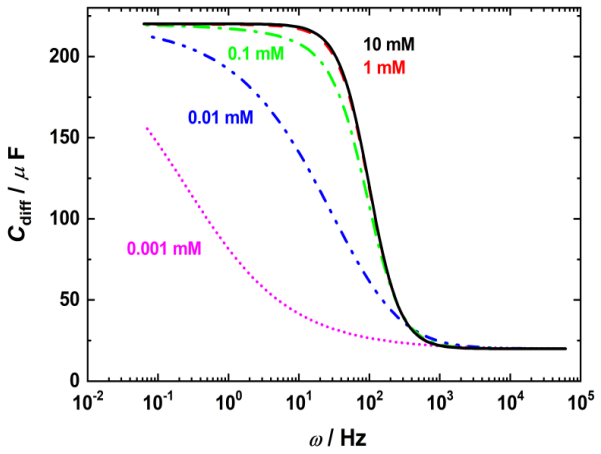

Figure 3. C_{diff} vs. ω dependences for equivalent circuit presented in Figure 1(b) for different concentrations of anions (values of C_{dl}, C_{ad}, R_{ad} are the same as in Figure 2)

It is seen that with the increase of Warburg constant σ (decrease of anion concentration) frequency range where C_{diff} represents the sum C_{dl} + C_{ad} moves towards lower values of $\omega$and onlyat concentration equal or higher than 10 mM mass-transport limitations are negligible for a given value of R_{ad} (in this case R_{ad} = 50 Ω should represent fast adsorption process). At lower concentrations than 1.0 mM low frequency plateau does not exist, indicating that in such a case even with the ideal, homogeneous electrode surface, real values of C_{diff}, as well as C_{dl} and C_{ad} from C_{diff} vs. ω curves, cannot be determined. It should be emphasized here that most of the C_{diff}vs. E curves [7] have been recorded for dilute solutions (concentration of anions lower than 1 mM) with high possibility for the adsorption reaction to be diffusion controlled and consequently with low possibility for C_{diff} to represent the sum C_{ad} + C_{dl}. C_{diff}vs. ω dependence for this equivalent circuit (Figure 1(b)) is given by the following equation

$$C_{diff} = C_{dl} + \frac{\omega C_{ad}(1+C_{ad}\sigma\omega^{1/2})}{(1+C_{ad}\sigma\omega^{1/2})^2+\omega^2 C_{ad}^2(R_{ct}+\sigma\omega^{1/2})^2} \qquad (4)$$

where σ represents Warburg coefficient

$$\sigma = \frac{RT}{z^2F^2c(2D)^{1/2}} \qquad (5)$$

(c and D are concentration and diffusion coefficient of anions respectively).

2.2. Real surface

Considering that even single crystal faces contain significant number of monoatomic terraces and cannot be considered as ideal, homogeneous surfaces (as shown by number of STM investigations [33]), introduction of *CPE* defined as $CPE = Z_{dl}(j\omega)^{-\alpha}$ [34]is inevitable in the interpretation of the double layer capacitance of atomically non-homogeneous surface. Let us consider two simplest cases:

(1) R_s and CPE_{dl} connected in series(without adsorption of anions) presented by the equivalent circuit shown in Figure 1(c). In this case the value of C_{diff}, independent of frequency for α= 1 and equal to the value of C_{dl}, becomes dependent on frequency with the decrease of αin the whole frequency range between $\omega = 10^{-2}$ Hz and $\omega = 10^{5}$ Hz. Hence, even if there is no adsorption on real surfaces, C_{diff} determined at one constant frequency cannot practically be used for determining C_{dl}.

(2) If for the case of simple anion adsorption, presented by the equivalent circuit shown in Figure 1(d), C_{dl} becomes replaced by CPE_{dl}, C_{diff}vs. $\omega$for such equivalent circuit is defined by the following equation

$$C_{diff} = C_{dl}{}^{*}\omega^{(\alpha-1)}\sin\left(\frac{\alpha\pi}{2}\right) + \frac{C_{ad}}{1+\omega^2 C_{ad}^2 R_{ad}^2} \qquad (6)$$

where $C_{dl}{}^{*}$represents constant in the $CPE_{dl}$with the dimensions F cm^{-2} s^{α}. In the presented equivalent circuit it is not possible to determine the value of C_{dl} since the value of C_{dl}could only be obtained for parallel connection or serial connection of $CPE_{dl}$and R. In the case of parallel connection of $CPE_{dl}$and $R$the value of C_{dl}could be obtained from the relation.

$$C_{dl} = \left[C_{dl}^{*}R^{(\alpha-1)}\right]^{\frac{1}{\alpha}} \qquad (7)$$

If $CPE_{dl}$and $R$are connected in series the value of C_{dl}could be obtained from the relation.

$$C_{dl} = \left[C_{dl}^{*}R^{(1-\alpha)}\right]^{\frac{1}{\alpha}} \qquad (8)$$

The influence of the value of α (heterogeneous character of the surface) on C_{diff} vs. ω diagrams is presented in Figure 4(a) and (b). Critical frequencies ω_c(ad) and ω_c(dl)could also be detected on this diagram. As can be seen the influence of the first part of equation (6) becomes significant already at α = 0.9 and, accordingly, determination of the real values of C_{ad} and C_{dl} at low and high frequencies, as it was the case for ideal surfaces, becomes impossible. Hence, to obtain the real values for the parameters of such equivalent circuit,C_{diff} vs. ω diagrams should be plotted for each potential and fitted by the equation (6).

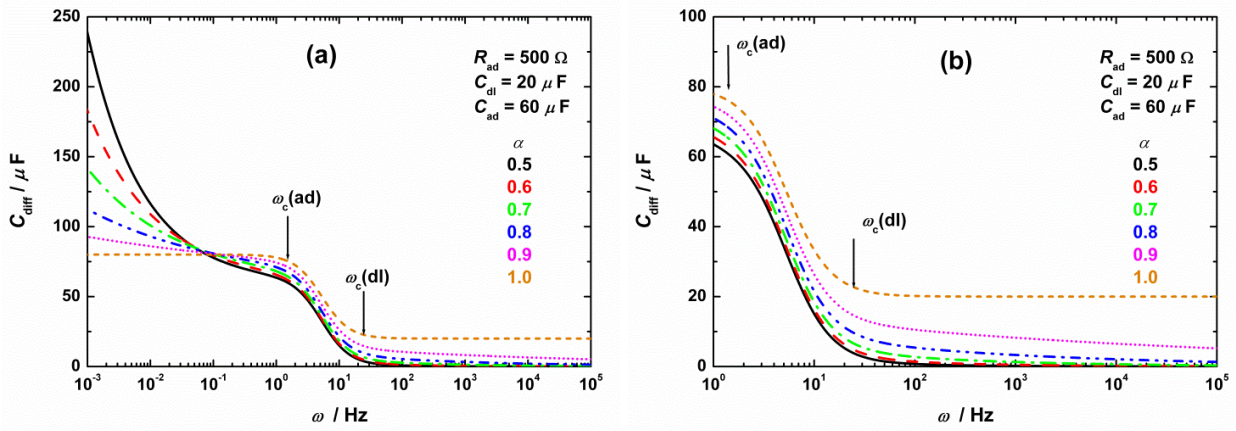

Figure 4. The influence of parameter α on the shape of C_{diff} vs. ωdependences for adsorption of anions on the real surfaces: (a) Whole frequency range; (b) High frequency range

2.3. Constant phase element (CPE)

Although the depression of the semi-circle in alternating current measurements, characteristic for the *CPE* behavior, was discovered in 1930-is in the presentation of imaginary vs. real component of dielectric constants in the so-called Cole-Cole plots [35], the first equation for *CPE* as a replacement for the capacitance in EIS measurements has been presented in the literature by Brug et al. [34] in 1984. The equation was based on the serial connection of R_s and *CPE*, while R_{ct} was simply added to the obtained equation being in parallel with the *CPE*. This new concept of C_{dl} on real electrode surfaces wasn't accepted immediately in the EIS measurements. The concept of *CPE*has been accepted in the EIS measurements about 10 years later. The first commercially available software for fitting EIS measurements was designed by Scribner and later by Solartron and

Gamry Instruments Inc. Much better fitting results were obtained with *CPE* in comparison with the fitting results obtained by using pure capacitance, represented by a parallel plate condenser. Since the *CPE* defines heterogeneity of the surface in the electrochemical EIS experiments and heterogeneity of the charge distribution at solid electrodes, it is reasonable to expect that better fit for real systems could be obtained by using CPE_{dl}instead of C_{dl}. The main problem in the use of commercially available software with *CPE* is the fact that the *CPE* constant (C_{dl}^*), obtained by fitting procedure, does not have the dimension of capacitance, i.e., F cm^{-2}, or Ω^{-1} cm^{-2} s, but its dimension is given in Ω^{-1} cm^{-2} s^{α}, where α is the exponent in the equation for the *CPE* ($Z_{CPE} = Z_{dl}(j\omega)^{-\alpha}$).

The definition of *CPE* has been discussed in several papers [36-44]. Hsu et al. [45] developed the equation for correction of capacitance to its real value, in the case of parallel connection between*CPE* and *R*, by using equation (9),

$$C_{dl} = C_{dl}^* (\omega''_{max})^{\alpha-1} \quad (9)$$

where ω''_{max} represents the frequency of the maximum on the $-Z''$ vs. ω dependence, which is independent of the exponent α [46], while C_{dl}^* represents a constant obtained by the fitting procedure. Another equation for obtaining the real value of capacitance from the *CPE* has been offered in the commercially available software (Gamry Instruments Inc., EIS 300, given by the equation (7)).

Hence, in order to obtain the real value ofC_{dl} it is necessary to know either of the two parameter values: ω''_{max} - frequency of the maximum on the $-Z''$ vs. ωcurve; or *R* – resistance connected in parallel with *CPE*.In both equations the physical meaning of CPE and *R* has been neglected. In many cases, for simple charge transfer reaction, *R* is a charge transfer resistance R_{ct} and it is reasonable to use R_{ct}in equation (7) for calculation of pure C_{dl}. Generally, in the brunch parallel to the *CPE* in the equivalent circuits representing different electrochemical processes only one resistance should exist to be used for calculation of $C_{dl}$by equation (7). If additional parameters, such as resistance of pores, or adsorption resistance, or adsorption capacitance, or else, are in the brunch parallel to the *CPE* in equivalent circuit, this procedure seems to be incorrectand the question arises could it be used to calculate C_{dl}? Another problem in calculation of C_{dl} by using ω''_{max} could be non-existence of the maximum on the $-Z''$ vs. ωcurve in the investigated frequency range?

Very often the R_s together with the R_{ct}had been used in the equation for the calculation of C_{dl}after applying commercial software for fitting EIS results in the literature. This procedure of C_{dl} calculationfrom CPE_{dl}has already been discussed and criticizedin the literature [47]. Hence, calculation of C_{dl} by using equations (7) or (9) is applicable for parallel connection of *CPE* and *R*only.

Recently, adsorption of iodide anions onto Ag(111) was investigated by fitting EIS results using commercial software and C_{diff}vs.ω dependence defined by equation (6) [48]. Significant difference in the obtained results has been detected, with those from C_{diff}vs.ω dependence analysis being more realistic. Most probably the reason for such difference was calculation of C_{dl} by using equation (7) expressed as

$$C_{dl} = [C_{dl}^* R_{ad}^{(\alpha-1)}]^{1/\alpha} \quad (10)$$

Hence, the statement that C_{dl}could be obtained from equation (7) only for*CPE* and *R* connected in parallel, without any additional parameter in the branch of equivalent circuit parallel to *CPE*, seems to be correct.

3. EXPERIMENTAL

All experiments were carried out in a two-compartment electrochemical cell at 25 ± 1 °C in an atmosphere of purified (99.999%) nitrogen. Ag(111) electrode (Monocrystals Company, d = 0.9 cm) was sealed in epoxy resin (resin EPON 828 + hardener TETA) in such a way that only the (111) disc surface was exposed to the solution. The surface area of the electrode exposed to electrolyte was 0.636 cm^2. The counter electrode was a platinum sheet and was placed parallel to the working electrode. The reference electrode was saturated calomel electrode (SCE). Reference electrode was placed in a separate compartment and connected to the working compartment by means of a Luggin capillary. Solution of 0.01 M NaCl was made from supra pure (99.999%) NaCl (Aldrich) and EASY pure UV water (Barnstead). All potentials are given vs. SCE.

Ag(111) was prepared by mechanical polishing procedure followed by chemical polishing in the solution containing NaCN and H_2O_2 as explained in a great details in one of our previous papers [49]. Before each experiment electrolyte was purged with high purity nitrogen (99.999%) for 45 min., while during the experiment nitrogen atmosphere was maintained over the solution to prevent contamination with oxygen.

Using universal programmer PAR M-175, potentiostat PAR M-173 and an X-Y recorder (Houston Instrument 2000R) CV experiments were

performed. FAS1Femtostat and Reference 600 potentiostatincluding software EIS3000 (Gamry Instruments Inc.) were used to perform EIS and C_{diff}measurements with an RMS amplitude of 5 mV and 10 points per decade. Single frequency, C_{diff} vs. *E*curves were obtained by measurements of real and imaginary component of impedance at constant frequency and potentialwith the potential being stepped in a sequence of 10 mV in the whole investigated potential range at different constant frequencies ranging from 0.1 Hz to 400 Hz. Measured values for the *Z'* were corrected for solution resistance (determined from the high frequency intercept on the *Z'* axis of *Z'*-*Z"* diagrams) and introduced into C_{diff}using eqn. (2).C_{diff} vs. ω dependences were fitted using non-linear curve fitting in Origin 2021.

4. RESULTS AND DISCUSSION

4.1. Ag(111), 0.01 M NaCl

CV recorded onto Ag(111) face in 0.01 M NaCl solution at the sweep rate of 100 mV s^{-1} is shown in Figure5. The CV is in good agreement with our previous results [9-11], as well as with the results of other authors [24,50-55]. As can be seen this CVis characterized by almost reversible pairs of two broad peaks (shoulders) at potentials of about –0.75 V and about –0.50 V respectively and by a pair of sharp peaks at the potential of about -0.03 V.Considering the shape of CV it appears that specific adsorption of anions starts already at potentials more positive than -0.8 V. In the potential region from -0.8 V to -0.4 V most probably two adsorption processes take place: (1) adsorption at the edge of monoatomic terraces and defects on the surface; (2) adsorption of anions at the flat part of monoatomic terraces (as shown in Figure 5). At potentials of the sharp peak (between -0.05 V and 0.0 V) phase transformation of anions adsorbed at the flat part of monoatomic terraces into $(\sqrt{3}\,x\,\sqrt{3})\mathrm{R30^o}$ [23-30] occurs. This ordered structure is presented in Figure 6. The anodic loop recorded at potential of 0.2 V corresponds to the formation of 3D AgCl [10]. If the anodic potential limit is low (as in the case of Figure 5) formation and dissolution of AgCl doesn't influence the shape of the CV, but for longer times of AgCl formation the layer of AgCl remains on the surface and the CV in the region of chloride anions adsorption changes with disappearance of characteristic peaks [10].

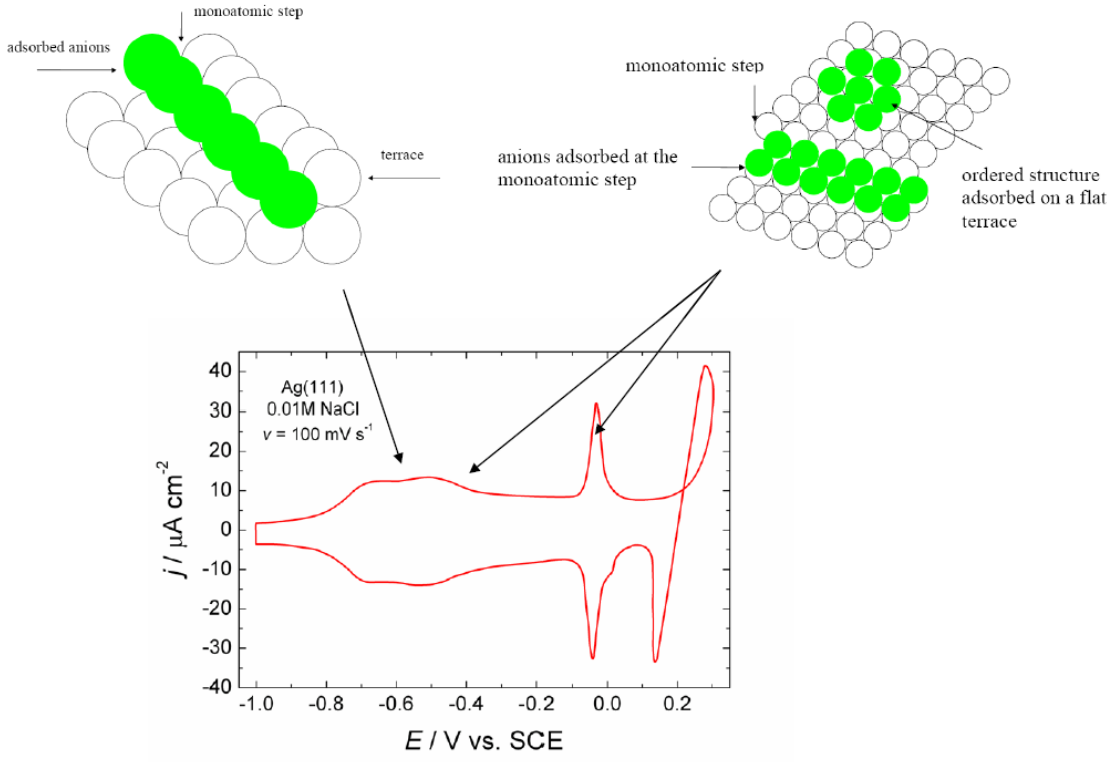

Figure 5. CV for Ag(111) recorded at the sweep rate of 100 mV s^{-1} in the solution of 0.01 M NaCl. Positions of adsorbed chloride anions are presented in upper part of the figure

Concerning R_{ad} it should be stated that this resistance represents a sum of two resistances: R_{ad}^{mt} – corresponding to the adsorption of anions at the edge of monoatomic terraces and defects on the surface and R_{ad}^{os} - corresponding to the adsorption of anions at the flat part of monoatomic

terraces, representing adsorption resistance for the formation of ordered structures. Unfortunately, these two resistances cannot be separated and determined independently, at least not by using equivalent circuit shown in Figure 1(d).

EIS measurements were performed in the frequency range from ~ 0.6 Hz to 1000 Hz at several constant potentials in the potential range from –1.0 Vto 0.05 V.

An attempt was made to fit Nyquist plots with the equivalent circuit presented in Figure 1 (d). Unfortunately it wasn't possible to get good fit of experimental results at any of the investigated potentials. This is due to the fact that employment of such a complicated combination of elements conduces to rather high correlation factors between the fitted values and accordingly the individual elements can only be determined with a large uncertainty [13]. Taking into account that commercial program for fitting impedance results by certain equivalent circuit is based on non-linear last square program that minimizes the sum of the $[(Z'-Z'_{calc})^2 + (Z''-Z''_{calc})^2]/AbsZ^2$and that only small part of the semi-circle on the Z'-Z'' diagrams exists, a bad fit of experimentally obtained results could be expected. At the same time the analysis presented by T. Pajkossy et al. [14], using complex plane C_{re} vs. C_{im} diagrams failed, most probably because of high concentration of chloride ions and the absence of diffusion limitations (see detailed explanation in Section 3.3.).

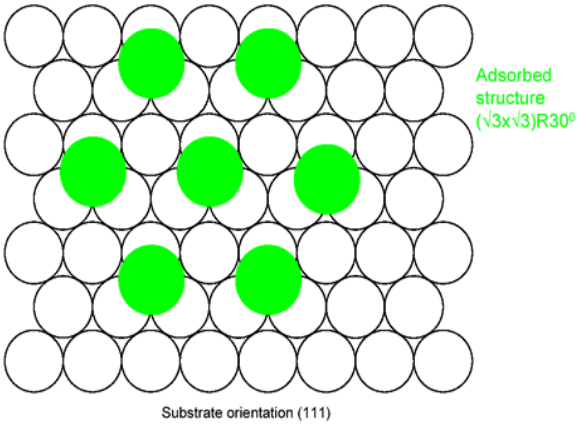

Figure 6. Schematic presentation of ordered structure adsorbed at potentials positive to the potential of sharp peaks on the CV. Assuming complete charge transfer between chloride anions and Ag(111) surface theoretical charge for this structure should be 74 $\mu C\ cm^{-2}$

Differential capacitance measurements (in steps of 10 mV, starting at –1.0 V and finishing at 0.05 V) were performed at following frequencies: 1000, 700, 400, 200, 100, 70, 40, 20, 10, 7, 4, 2, 1, 0.7, 0.4, 0.2 and 0.1 Hz. Corrected values for differential capacitance were obtained by using equation (3) and corresponding values of Z'_{corr} and Z'' detected in these experiments. Some of the obtained C_{diff} vs. E curves are shown in Figure 7. It is interesting to note that almost identical diagrams were obtained at frequencies lower than 1 Hz, while C_{diff} was found to decrease with increasing frequency. Presented results indicate that the measurement of C_{diff} at a constant frequency is not sufficient for determining the parameters of chloride anions adsorption, although the shape of the C_{diff} vs. E curves recorded at frequencies lower than 10 Hz is practically identical to the shape of CV.

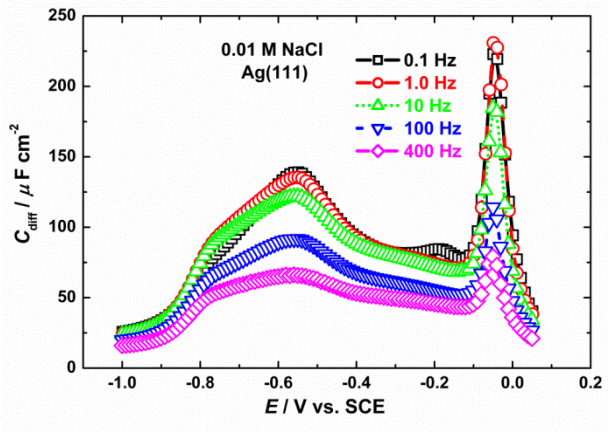

Figure 7. C_{diff} vs. E curves recorded at different frequencies (designated in the figure)

C_{diff} vs. E curves recorded at the frequency of 1 Hz by changing potential in both directions, from –1.0 V to 0.05 V and back were found to be identical, indicating high reversibility and stability of the system.Considering results of in situ X-ray investigations of anion adsorption [26-30], it seems reasonable to assume that partial charge transfer occurs during this process and that equivalent circuit presented in Figure 1(d) should be used for the analysis of the obtained results.

C_{diff} vs. ω curves were plotted at each applied potential. In the potential range between –1.0 V and –0.5 V this has been done in steps of 100 mV, from -0.5 V to -0.1 V in steps of 50 mV, while in the region of sharp peak on C_{diff} vs. E curves this was done in the sequence of 10 mV. In order to obtain values for C_{dl}, C_{ad}, R_{ad} and α, fitting of C_{diff} vs. ω curves has been performed by using equation (6). AllC_{diff} vs. ω curves are presented in Figure8 (a,b,c). Experimental points are presented by squares, circles, triangles, etc., while the lines represent fitting curves. Potentials are designated in the figure for each curve. As can be seen very good fits have been obtained.

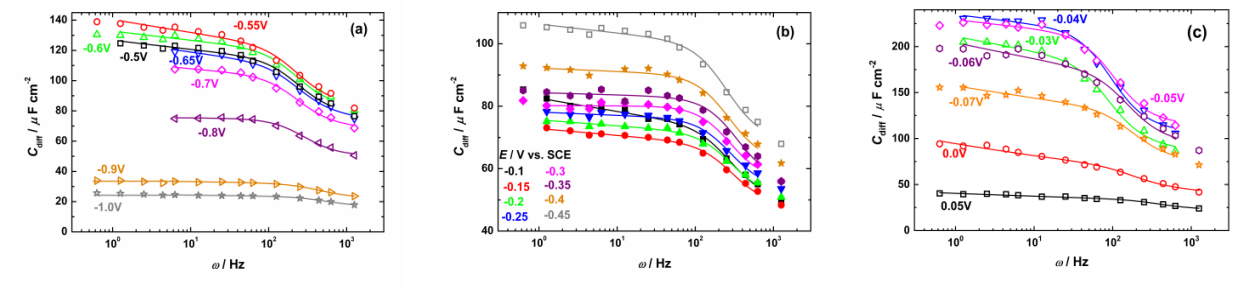

Figure 8. C_{diff} vs. ω curves for all applied potentials (designated in the figure)

The values of C_{dl}^*, C_{ad}, R_{ad} and α obtained by fitting procedure were used to plot C_{ad} vs. E, R_{ad} vs. E, and αvs. $E$and C_{dl}^* vs. Ecurves. Obtained dependences are presented in Figure 9 (a-d).

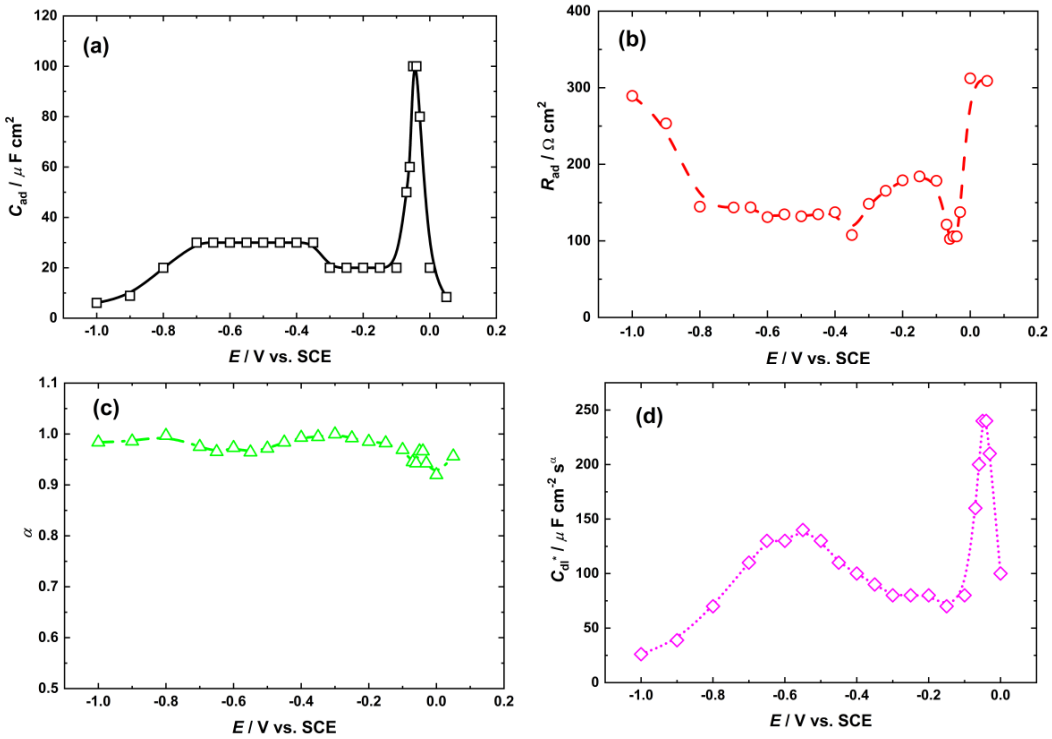

Figure 9. (a) C_{ad} vs. E,(b) R_{ad} vs. E curve, (c) α vs. E curve, C_{ad} vs. E andC_{dl}^* vs. E curves

By using analysis presented in this work C_{dl}^* values were found to be higher than those of C_{ad}. Relatively high values of the double layer capacitance (about 50 μF cm^{-2}), dependent on potential, were detected in the work of T. Pajkossy et al. [14] in the case of bromide adsorption on gold single crystals, with the adsorption capacitance being much higher, but they used 0.1 M $HClO_4$ as a supporting electrolyte with only 0.15 mM of NaBr as adsorbing substance. Considering contribution of the double layer capacitance to the total capacitance of the system, one would expect increase of double layer capacitance with increasing concentration of electrolyte, since more anions should be incorporated in the inner layer and adsorbed at the surface at higher concentrations. It is interesting to note that the charge under C_{ad} vs. E curve amounts to 27μC cm^{-2}. Taking into account significant number of steps and terraces present on the single crystal surfaces [33] one can assume that higher amount of charge than that needed for $(\sqrt{3}\,x\,\sqrt{3})$R30°adsorbed structure of chloride anions (detected by different techniques for this system [23-25]) should be obtained. Hence, one can conclude that because of adsorption of chloride anions at kinks and steps, this structure can be formed by complete charge transfer between chloride anions and silver surface. Since the double layer capacitance by definition represents purely capacitive component of total electrode capacitance, it appears that only charge under the C_{ad} vs. E curve can be involved in the

adsorption of $(\sqrt{3}\,x\,\sqrt{3})$R30° structure**.** The value of charge under the C_{ad} vs. *E*curveof 27 μC cm^{-2}indicates that partial charge transfer is involved to some extent in the process of$(\sqrt{3}\,x\,\sqrt{3})$R30° structure formation, since for complete charge transfer between chloride anions and Ag(111) for the formation of this ordered structure amounts to 74 μC cm^{-2}. This is in contradiction with our previous results [9-11] that complete charge transfer occurs during the formation of this structure, most probably as a consequence of different approaches used in previous and present work. It seems that considering total charge under the CV, or under the C_{diff} vs. *E* curve, or under the *Q* vs. *E* curve obtained by pulse experiments and subtracting the double layer charge assuming linear increase of Q_{dl} with potential (as has been done in previous paper [10]) is not correct approach, since it is obvious that Q_{dl} does not change linearly with potential, i.e. C_{dl} is not constant over the whole potential range. Accordingly, the charge associated with adsorption should be determined under the C_{ad} vs. *E* curves only. Hence, one can conclude that approach presented in this work seems to be more reliable.

Some interesting features of these results deserve further discussion. The first one is the fact that even in the potential range of "double layer behavior" (between –1.0 V and –0.8 V on the CV shown in Figure5) C_{diff} vs. ω curvesare characterized by the presence of one inflection point (Figure 8(a)), indicating the presence of C_{ad} and R_{ad}.

Considering R_{ad} vs. *E* dependence (Figure 8(b)) it appears that its shape is opposite to the one for C_{ad} vs. *E* dependence (Figure 8(a)), indicating faster adsorption (lower R_{ad}) in the potential region of higher values of C_{ad}, with the minimum being exactly at the potential of sharp peak on the C_{ad} vs. *E* dependence.

Another interesting feature of this approach is α vs. *E* dependence shown in Figure 8(c). The value of $\alpha$is seen to be close to 1 up to the potential of ordered structure formation. Although the value of $C_{dl}$is changing significantly with the potential, it appears that the homogeneity of the Ag(111) surface remains practically constant, i.e. adsorbed anions only slightly change the charge distribution at the potential of ordered structure formation.

4.2. Ag(100), 0.01 M KBr

CV recorded onto Ag(100) face in 0.01 M KBr solution at the sweep rate of 20 mV s^{-1} is shown in Figure10. This CV is characterized by reversible pair of broad peaks (shoulders) at potential of about –1.1 V and by one pair of sharp peaks at the potential of about -0.7 V.According to theX-ray scattering (SXS) results [29] in the case of bromide adsorption onto Ag(100) ordered c(2x2) structure has been formed, with the charge number being –0.85±0.05 at constant chemical potential, indicating also existence of partial charge transfer between adsorbed anions and the substrate. The charge density for the formation of ordered c(2x2) structure, determined from the C_{diff} vs. *E* curve at single frequency of 18 Hz, was fund to be 43 – 50 μC cm^{-2}.

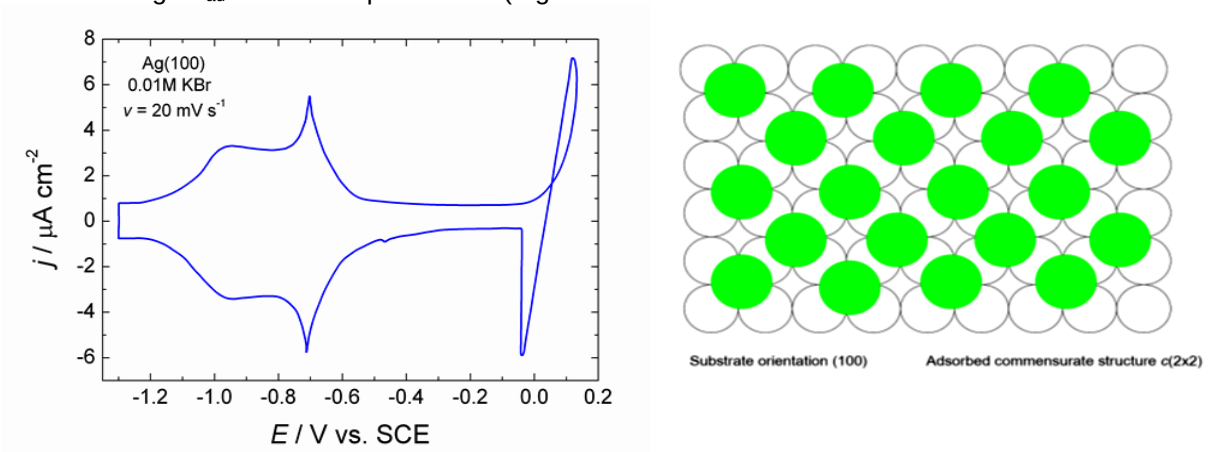

Figure 10. CV recorded onto Ag(100) in 0.01 M KBr solution at the sweep rate of 20 mV s^{-1} (left) and ordered c(2x2) structure of adsorbed bromide anions (right)

Differential capacitance measurements (in steps of 10 mV, starting at –1.2 V and finishing at -0.1 V) were performed at following frequencies: 1000, 700, 400, 200, 100, 70, 40, 20, 10, 7, 4, 2, 1, 0.7, 0.4, 0.2 and 0.1 Hz. Corrected values for differential capacitance were obtained by using equation (3) and corresponding values of Z'_{corr} and *Z''* detected in these experiments. Some of the obtained C_{diff} vs. *E* curves are shown in Figure 11. At frequencies lower than 10 Hz the shape of C_{diff} vs. *E* curves is practically identical to the CV and the same stability as in the case of adsorption of

chloride anions onto Ag(111) has been detected (C_{diff} vs. E curves obtained by changing potential from -1.2 V to -0.1 V and back at the frequency of 0.1 Hz were identical).

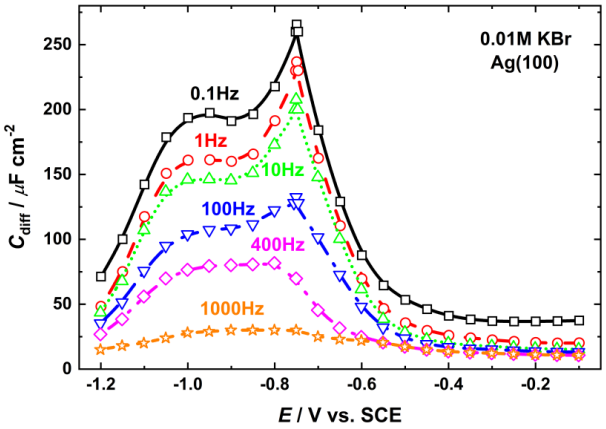

Figure 11. C_{diff} vs. E curves recorded at different frequencies (designated in the figure)

C_{diff} vs. ω curves were recorded in steps of 100 mV, while the values for C_{dl}^*, C_{ad}, R_{ad} and α were obtained by fitting of C_{diff} vs. ωdependences using equation (6). AllC_{diff} vs. ω curves are presented in Figure12 (a,b). Experimental points are presented by squares, circles, triangles, etc., while the lines represent fitting curves. Potentials are designated in the figure for each curve. As for Ag(111) in 0.01 M NaCl very good fits have been obtained, but the shapes of C_{diff} vs. ω curves were different. In the potential region of random adsorption (at the terraces)and formation of ordered c(2x2) structure (from -1.2 V to -0.6 V, Figure 12(a)) C_{diff} vs. ω curves were characterized by the inflection point, most probably corresponding to ω_c(ad) (see Figures 2(a) and 4), while in the potential region with adsorption onto ordered bromide anions structure (Figure 12 (b)) most of the curves correspond to the exponential increase of C_{diff}. This indicates that for those potentials ω_c(ad) has been passed and these curves correspond to the part of the C_{diff} vs. ω curves were C_{diff} exponentially increases (see Figure 4).

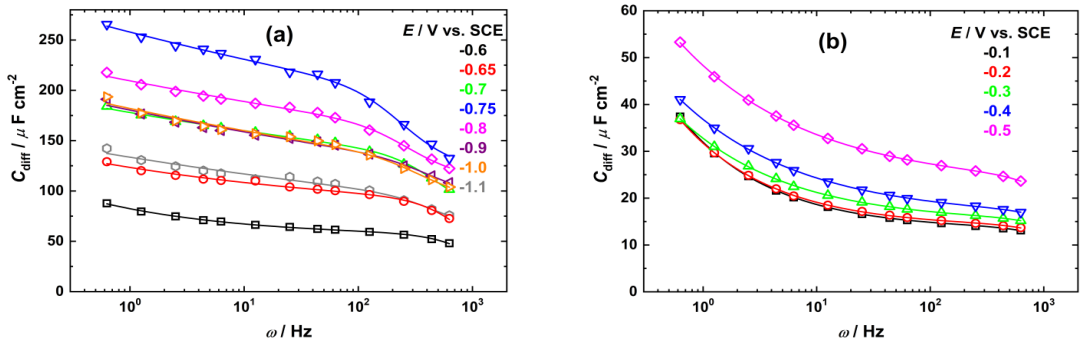

Figure 12. C_{diff} vs. ω curves for all applied potentials (designated in the figure)

The values of C_{dl}^*, C_{ad}, R_{ad} and α obtained by fitting procedure were used to plot C_{ad} vs. E, R_{ad} vs. E, C_{dl} vs. E,αvs. E and C_{dl}^* vs. Ecurves. Obtained dependences are presented in Figure 13 (a-d).

The shape ofC_{dl}^* vs. Ecurveis practically identical to the shape of C_{diff} vs. E curves obtained at low frequencies and the shape of CV, while the shape of C_{ad} vs. E curve is slightly different with two maxima in the potential range of ordered structure adsorption (Figure 13(a)). Considering R_{ad} vs. E curve (Figure 13(b)) sharp decrease of R_{ad}in the potential region of ordered structure adsorption indicates fast adsorption of bromide anions during this process, reaching minimum at the potential where ordered structure is completed. Slight increase of R_{ad} at more positive potentials, as well as slight decrease of C_{ad}, indicate that adsorption didn't stop and that it continues after ordered structure is completed. This is in accordance with the findings of chronocoulometry curves presented in Ref. [29], where the charge for bromide anions adsorption continuously increased, changing slope after ordered structure has been completed and reaching maximum at about 75 μC cm^{-2}. According to the explanation given in Ref. [29] for the (SXS) results, "This result demonstrates that a significant percentage of the bromide scattering amplitude within the disordered region is out-of-phase with that of the substrate. This out-of-phase condition occurs when the bromide ions are adsorbed in the fourfold hollow sites of the substrate", it is obvious that adsorption of bromide anions continues after the ordered structure is formed. This is also in accordance with the change of α with E (Figure 13(c)). After the formation of ordered structure α sharply decreases and the surface becomes quite heterogeneous due to further adsorption of bromide anions, being confirmed by the change of the shape of C_{diff} vs. ω curves (at lower α values C_{diff} exponentially increases - see Figures 4 and 12(b)). Finally, the charge under the C_{ad} vs. E curve of 31 μC cm^{-2} confirms that only partial charge transfer between bromide anions and Ag(100) occurs.

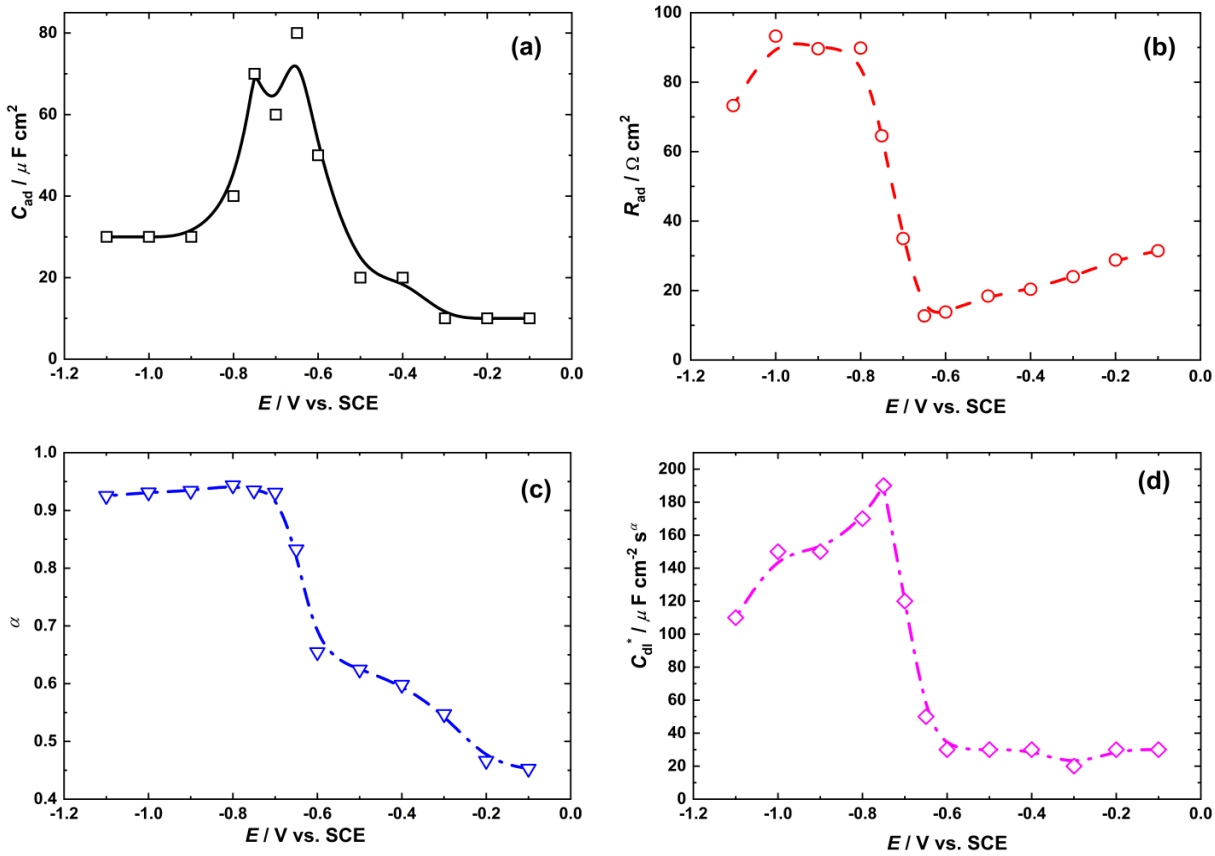

Figure 13. (a) C_{ad} vs. E,(b) R_{ad} vs. E, (c) α vs. E and C_{dl}^{*}vs. E curves

4.3. Polycrystalline Ag, 0.1 M $NaClO_4$ + 0.01 M KBr

CV recorded onto polycrystalline Ag in 0.1 M $NaClO_4$ + 0.01 M KBr solution at the sweep rate of 100 mV s^{-1} is shown in Figure14. Since two anions are present in the solution it is possible that both anions adsorb. Since perchlorate is a big anion with tetrahedral structure its adsorption should be week and peaks of adsorption mostly correspond to the bromide anion. Adsorption of bromide is characterized by a broad peak between -0.9 V and -0.4 V and two small peaks at potential more positive than -0.2 V, before the formation of 3D AgBr characterized by a crystallization loop. As shown by Endo et al. [30],using the same solution as in this experiment, adsorption of bromide at Ag(111) occurs through a broad peak at more negative potentials and sharp peak at about 0.05 V vs. Ag/AgCl. Sharp peak is ascribed to the phase transition (surface transformation) of adsorbed layer and formation of AgBr(111) layer without any change in the charge, or without additional adsorption of bromide (change of the surface Br density). Actually they suggested oxidation of silver atoms to form AgBr(111) monolayer. Since at more positive potentials the formation of 3D AgBroccurs (as is the case for 3D AgCl), this might be the first step, formation of 2DAgBr layer, in the process of the formation of 3DAgBr. Of course, this could be seen on the surface of single crystal (111) face, but it is practically impossible to obtain such peaks at the polycrystalline surface. Hence, two small peaks just before the formation of 3D AgBr could correspond to the process of adsorbed layer transformation.

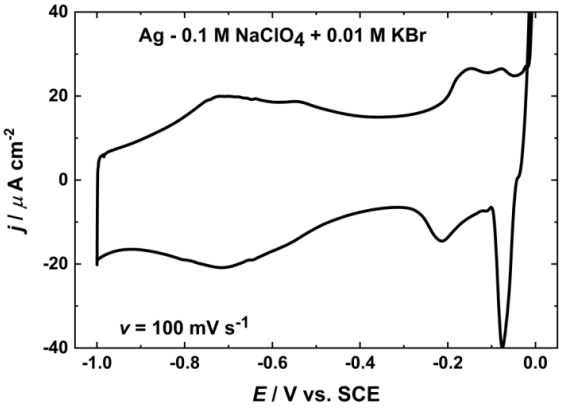

Figure 14. CV recorded onto polycrystalline Ag in 0.1 M $NaClO_4$ + 0.01 M KBr solution at the sweep rate of 100 mV s^{-1}

4.3.1. EIS measurements

The process of bromide adsorption on the polycrystalline silver has been investigated by EIS measurements in the frequency range from 100 kHz to 0.01 Hz and an attempt to fit obtained results either in a form of Nyquist, or Bode diagrams, or by fitting Z' vs. ω and $-Z''$ vs. ω dependences has been made. In this case fitting of Z' vs. ω and $-Z''$ vs. ω dependences has been performed since these dependences were later used for plotting C_{diff} vs. ω curves, as was the case in previous experiments on Ag(111) and Ag(100). As already discussed in Section 2.3. and in Ref. [13], the use of commercial software does not provide the possibility to obtain the value of C_{dl}(only Y_{dl} constant could be obtained), but the values of C_{ad} and R_{ad} should be precisely determined.

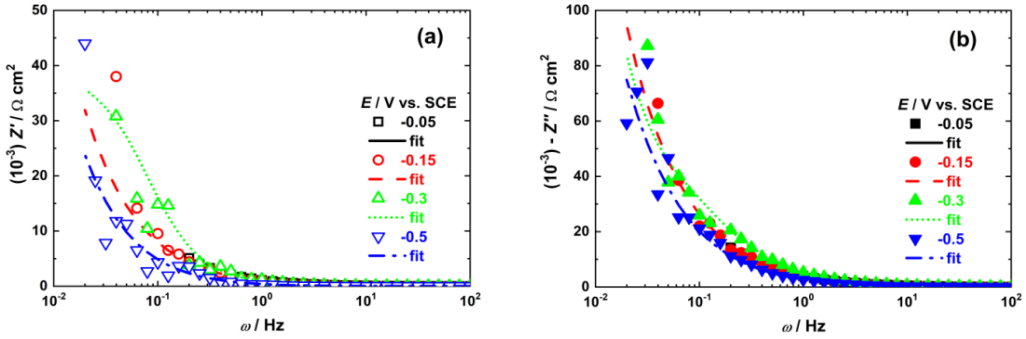

Figure 15. Z' vs. ω (a) and -Z" vs. ω (b) dependences obtained by EIS measurements and fitted by the equivalent circuit presented in Figure 1(d) using commercial software EIS 300. Potentials at which the measurements were performed are designated in the figure

Hence, Z' vs. ω and $-Z''$ vs. ω dependences were obtained by EIS 300 software and fitted by the equivalent circuit presented in Figure 1(d). Obtained results for several potentials are presented in Figure 15. It could be seen that experimental points deviate from the fitting lines, particularly in the low frequency range. Although the "goodness of fit" was much higher than 1 x 10^{-4} (acceptable limit of the "goodness of fit"), equivalent circuit parameters, C_{ad}, R_{ad} and α obtained by fitting procedure are determined and presented in Figure 16. Considering shape of CV in Figure 14, the shapes of C_{ad} vs. E, R_{ad} vs. E and α vs. E dependences are not in agreement with the CV, indicating that fitting procedure using commercial software is not suitable for such equivalent circuit. At the same time the values of $R_{ad}$was found to vary for six orders of magnitude.

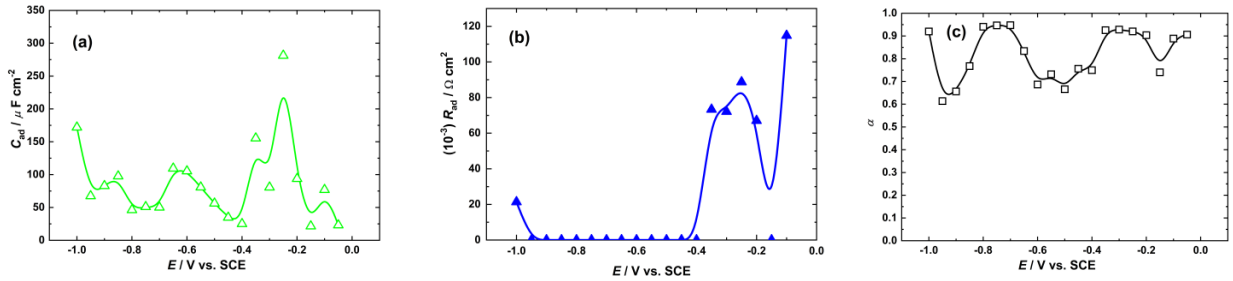

Figure 16. C_{ad} vs. E (a), R_{ad} vs. E (b) and α vs. E (c) dependences obtained by fitting procedure using commercial software

4.3.2. C_{diff} vs. ω dependences

In order to obtain good fits lower frequency limit was set at 1 Hz, while high frequency limit was in most cases 1000 Hz. C_{diff} vs. ωdependences were recorded from -1.0 V to -0.05 V in steps of 50 mV and fitted with equation (6). Results for all applied potentials are presented in Figure 17 (a),(b),(c).According to the presented results fitting procedure was extremely accurate, i.e. there was no deviation of experimental points from the fitting lines.

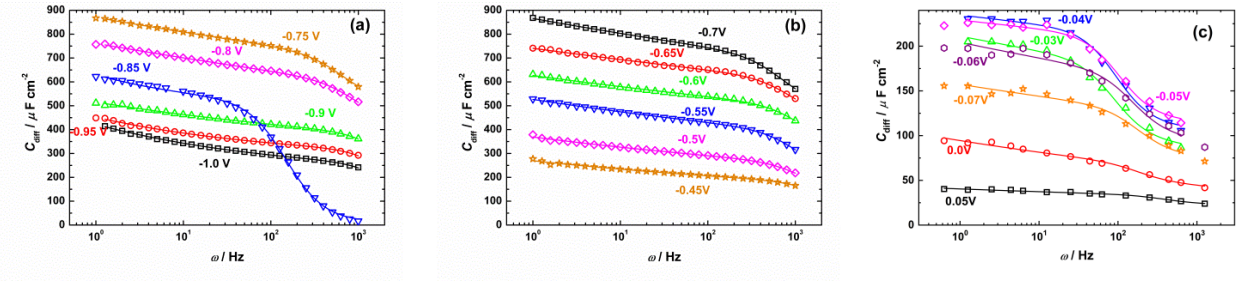

Figure 17. C_{diff} vs. ω curves for all applied potentials (designated in the figure)

Obtained values for C_{dl}^*, C_{ad}, R_{ad} and α are plotted as a function of potential in Figure 18. In comparison with the Figure 16 quite different results were obtained by fitting C_{diff} vs. ωdependences, being in accordance with the shape of CV curve (Figure 14). Since on the polycrystalline silver number of irregularities (kinks, steps, etc.) on the surface is much higher the formation of any ordered structure is impossible. Peaks of high values of capacitance on C_{dl}^* vs. E(Figure 18(d)) and C_{ad} vs. E curves (Figure 18 (a)) appearing in the region of broad adsorption peak on the CV indicate adsorption of large amount of bromide anions. At more positive potentials small adsorption peaks confirm further adsorption of much smaller amount of bromide anions. Considering R_{ad} vs. E curve it could be stated that adsorption is fast (low value of R_{ad}), while in the results of fitting with the commercial software the values of R_{ad} were extremely high. Dependence of αon potential (Figure 18(c)) indicates that with the beginning of adsorption of bromide anions the surface becomes more homogeneous (surface defects become covered with the anions) up to the point (-0.4 V) where adsorption deceases and $\alpha$is characterized by the minimum. At more positive potentials increase ofαvalue indicates rearrangement of the electrode surface causing more homogeneous one with a higher value of α. The amount of charge under the C_{ad} vs. E curve of 151 μC cm^{-2} seems to be reasonable considering surface roughness of chemically polished polycrystalline silver electrode.

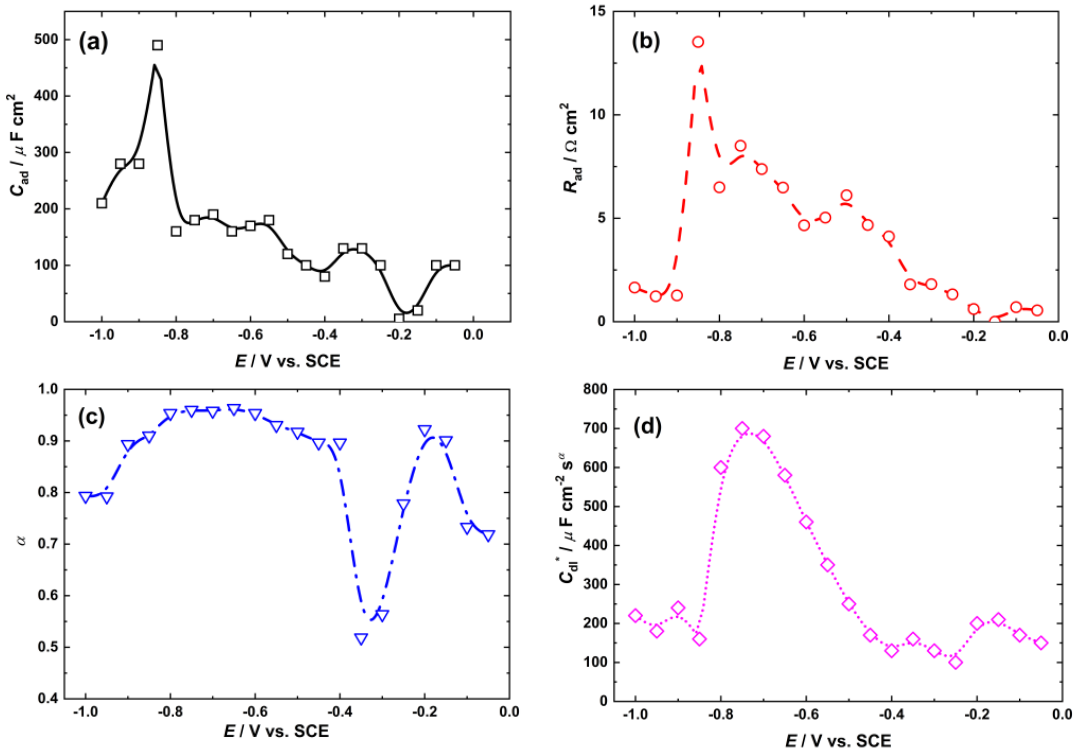

Figure 18. (a) C_{ad} vs. E,(b) R_{ad} vs. E, (c) α vs. E and C_{dl}^* vs. E curves

Considering explanation of fitting procedure presented at the web-site of Gamry Instruments Inc. under the link Gamry.com/application-notes/Electrochemical Impedance Spectroscopy/fit-in-eis (Qualyty of Your Fit in EIS) it appears that "*The most important of these layers of fitting is the representation of a real physical system. Second most important is being sure that the error bar for each ideal component in the model is smaller than the value calculated for that component, and that any residual errors are not systematic, but random. The least important of all is the goodness of fit, or* χ^2 *value. The basic rule is:* ***Use the simplest model to fit the data.***" Below are presented two extreme examples of Tables with the fitting results for two different potentials. In Table 1 Errors for all parameters are lower than the value of Parameters, indicating good fit. In Table 2 the value of Error for R_{ad} is extremely high (for six orders of magnitude higher than the value of R_{ad}). Fitting was performed at 20 different potentials and only in 6 cases (at six potentials) Errors for R_{ad} were significantly higher than the Parameter. Corresponding fractional residual errors are presented in Figures 19 and 20 respectively. As can be seen fractional residual errors are not systematic and become pronounced at frequencies lower than 1 Hz. Hence, in most measurements fits should be considered as good. It is interesting to note that only R_{ad} showed high values of Error, indicating low sensitivity to the fitting procedure.

Table 1.

Parameter	Value	±Error	Units
Rs	6.404	55.82e-3	ohm
Ydl	100.9e-6	1.168e-6	S*s^a
adl	919.9e-3	2.273e-3	
Cad	171.9e-6	16.47e-6	F
Rad	21.36e3	859.1	ohm
Goodness of Fit	677.8e-6		
-1.0 V.DTA			

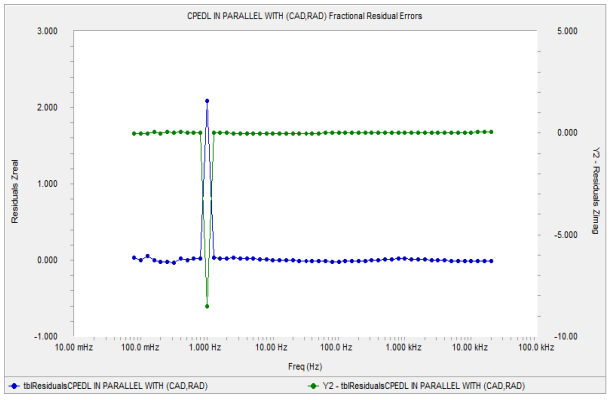

Figure 19. Fractional residual errors for results presented in Table 1

Table 2.

Parameter	Value	±Error	Units
Rs	6.856	1.823	ohm
Ydl	48.68e-6	2.520e-6	S*s^a
adl	686.7e-3	20.90e-3	
Cad	105.3e-6	2.182e-6	F
Rad	986.7e-9	1.908	ohm
Goodness of Fit	7.228e-3		
-0.6 V.DTA			

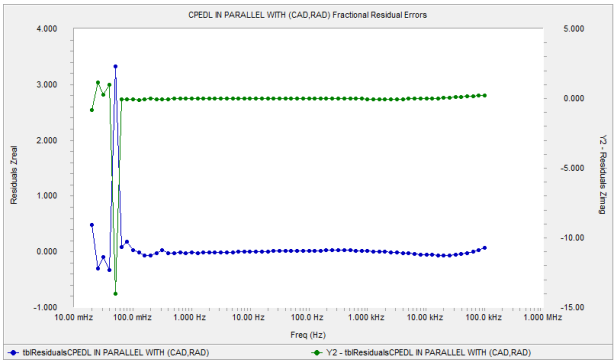

Figure 20. Fractional residual errors for results presented in Table 2

In the case of fitting C_{diff} vs. ω curves perfect fits were obtained with the non-linear curve fitting using Origin 2021. For all investigated potentials similar values for Chi^2/DoF and R^2 were obtained (one example Chi^2/DoF = 3.415 x 10^{-13} and R^2= 0.9985).

The question arises what is the reason for the difference in the fitting procedures used in this work. The only reasonable explanation is the fact that in the case of commercial fitting two functions are fitted simultaneously, *Z'* vs. ω and *-Z''* vs. ω, while for C_{diff} vs. ω curves only one function is fitted. Hence, it seems that for the adsorption of anions using simple equivalent circuit presented in Figure 1(d), C_{diff} vs. ω curves, obtained from the dependences *Z'* vs. ω and *-Z''* vs. ω, should be considered since their fitting produces more precise and more realistic values for parameters C_{dl}^*, C_{ad}, R_{ad} and α.

5. CONCLUSIONS

Several equivalent circuits for simulating adsorption of anions for ideal and real surfaces are presented and discussed.

Analysis of C_{diff} vs. ω curves simulated for different equivalent circuits, representing different cases of anion adsorption, has shown that in all cases with ideal, homogeneous electrode surface, part of the C_{diff} vs. ω curves between critical frequencies ω_c(dl) and ω_c(ad) cannot be used for

determining the real values of C_{dl} and C_{ad}. C_{diff} is equal to C_{dl} at frequencies higher than ω_c(dl), while C_{dl} + C_{ad} is equal to C_{diff} at frequencies lower than ω_c(ad). At the same time the positions of ω_c(dl) and ω_c(ad) on the C_{diff} vs. ω curves depend on the values of C_{ad} and R_{ad} and if R_{ad} is very high (slow adsorption process) the value of C_{ad} cannot be determined from the C_{diff} vs. ω curves in the range of frequencies available in EIS measurements (lower frequency limit is 0.01 Hz).

In the case of diffusion control of anion adsorption at ideal surface (the concentration of anions lower than 1 mM) the value of C_{ad} cannot be determined from C_{diff} vs. ω curves.

C_{diff} vs. *E*dependences recorded at a single frequency cannot be used for determining parameters of anions adsorption.

To obtain the values of C_{dl}, $C_{ad}$and R_{ad} for real surfaces it is mandatory to plot C_{diff} vs. ω curve for each applied potential and fit this curve with the equation (6). Fitting of Nyquist, or Bode plots, or *Z*' vs. ω and -*Z*'' vs. ω dependences with the equivalent circuit composed of CPE_{dl} connected in parallel with $C_{ad}$and R_{ad} using commercially available software is not recommended, not only because of low precision, but also because of impossibility to determine the value of C_{dl}.

The statement of point 5 has been confirmed for three cases. Chloride adsorption onto Ag(111), bromide adsorption onto Ag(100) and bromide adsorption onto polycrystalline Ag. In all cases C_{diff} vs. ω curves were recorded at constant potentials and fitted with the equation (6). C_{ad} vs. *E*, C_{dl} vs. *E*,C_{dl} + C_{ad} vs. *E*, R_{ad} vs. *E*, and ωvs. *E* curves confirmed that the used equivalent circuit is suitable for presenting adsorption of anions. In all cases the amount of charge under the C_{ad} vs. *E* curves indicated partial charge transfer between the anions and substrate during the anions adsorption.

Finally, explanation for significant difference in the results of both fitting procedures, for the first time presented in the literature, is very simple: in the case of commercial fitting two functions (*Z*' vs. ω and -*Z*'' vs. ω) are fitted simultaneously, while in the case of C_{diff} vs. ωdependences only one function is fitted, producing more accurate results for the parameters of the equivalent circuit.

6. REFERENCES

[1] D.C. Grahame (1954) Differential Capacity of Mercury in Aqueous Sodium Fluoride Solutions. I. Effect of Concentration at 25°, J. Am. Chem. Soc., 76, 4819-4823. https://doi.org/10.1021/ja01648a014

[2] R. Reeves, The Double Layer in the Absence of Specific Adsorption,in: J. O'M. Bockris, B.E. Conway, E. Yeager(Eds.), Comprehensive Treatise of Electrochemistry, vol. 1, Plenum, New York and London, 1980, Chapter 3, pp. 83-134.

[3] G. Valette, A. Hamelin (1973) Structure et propriétés de la couche double électrochimique à l'interphase argent/solutions aqueuses de fluorure de sodium, J. Electroanal. Chem. 45, 301-319. https://doi.org/10.1016/S0022-0728(73)80166-4

[4] D. Henderson, L. Blum (1982) A simple theory of the electric double layer including solvent effects, J. Electroanal. Chem., 132, 1-13. https://doi.org/10.1016/0022-0728(82)85001-8

[5] D. Henderson (1983) Recent progress in the theory of the electric double layer, Progress Surf. Sci., 13, 197-224. https://doi.org/10.1016/0079-6816(83)90004-7

[6] G. Valette (1982) Double layer on silver single crystal electrodes in contact with electrolytes having anions which are slightly specifically adsorbed: Part II. The (100) face,J. Electroanal. Chem., 138, 37-54. https://doi.org/10.1016/0022-0728(82)87126-X

[7] A. Hamelin, Double-layer properties at *sp*and *sd*metal single-crystal electrodes, in: B. E. Conway, J. O'M. Bockris, R. White (Eds.), Modern Aspects of Electrochemistry, vol. 16, Plenum, New York, 1985, Chapter 1.

[8] V.D. Jović, B.M. Jović, R. Parsons (1990)Acetate adsorption on the (111) oriented silver single crystal surface, J. Electroanal. Chem.,290, 251-262. https://doi.org/10.1016/0022-0728(90)87435-M

[9] V.D. Jović, R. Parsons, B.M. Jović (1992) Anion absorption on the (111) face of silver, J. Electroanal. Chem. 339, 327-337. https://doi.org/10.1016/0022-0728(92)80461-C

[10] V.D. Jović, B.M. Jović (2003) EIS and differential capacitance measurements onto single crystal faces in different solutions. Part I - Ag(111) in 0.01MNaCl, J. Electroanal. Chem., 541, 1-11. https://doi.org/10.1016/S0022-0728(02)01309-8

[11] B.M. Jović, V.D. Jović, D.M. Dražić(1995)Kinetics of chloride ion adsorption and the mechanism of AgCl layer formation on the (111), (100) and (110) faces of silver, J. Electroanal. Chem., 399, 197-206. https://doi.org/10.1016/0022-0728(95)04291-1

[12] S. Härtinger, K. Doblhofer (1995) The electro-chemical interface between copper (111) and aqueous electrolytes, J. Electroanal. Chem., 380, 185-191. https://doi.org/10.1016/0022-0728(94)03650-R

[13] D. Eberhardt, E. Santos, W. Schmickler (1996) Impedance studies of reconstructed and non-reconstructed gold single crystal surfaces, J. Electroanal. Chem., 419, 23-31. https://doi.org/10.1016/S0022-0728(96)04872-3

[14] T. Pajkossy, T. Wandlowski, D.M. Kolb (1996) Impedance aspects of anion adsorption on gold single crystal electrodes, J. Electroanal. Chem., 414, 209-220. https://doi.org/10.1016/0022-0728(96)04700-6

[15] M. Sluyters-Rehbach, J. Sluyters, in A. Bard (ed.), Electroanalytical Chemistry, vol. 4, Marcel Dekker, New York, 1970, pp. 75-80.

[16] Z. Kerner, T.Pajkossy (2000) On the origin of capacitance dispersion of rough electrodes, Electrochim. Acta, 46, 207-211. https://doi.org/10.1016/S0013-4686(00)00574-0

[17] R. de Levi, Electrochemical response of porous and rough electrodes, in: P. Delaney, Ch. W. Tobias (Eds.), Advances in Electrochemical Engineering, vol. 6, Wiley, New York, 1967.

[18] O. S. Ksenzhek, V. V. Stender (1956) Dokl. Akad. NaukSSSR, 106, 487.

[19] O. S. Ksenzhek, V. V. Stender (1957)Zh. Fiz. Khim., 31, 117.

[20] R. de Levi (1963) On porous electrodes in electrolyte solutions*,Electrochim. Acta, 8, 751-780. https://doi.org/10.1016/0013-4686(63)80042-0

[21] T. Pajkossy (1997) Capacitance dispersion on solid electrodes: anion adsorption studies on gold single crystal electrodes, Solid State Ionics, 94, 123-129. https://doi.org/10.1016/S0167-2738(96)00507-3

[22] T. Pajkossy (1994) Impedance of rough capacitive electrodes, J. Electroanal. Chem., 364, 111-125. https://doi.org/10.1016/0022-0728(93)02949-I

[23] G.N. Salaita, F. Lu, L. Laguren-Davison, A.T. Hubbard (1987) Structure and composition of the Ag (111) surface as a function of electrode potential in aqueous halide solutions, J. Electroanal. Chem., 229, 1-17. https://doi.org/10.1016/0022-0728(87)85127-6

[24] M.S. Zei (1991) The structure of halide adlayers on Ag (111) electrodes, J.Electroanal.Chem., 308, 295-307. https://doi.org/10.1016/0022-0728(91)85074-Y

[25] G. Aloisi, A.M. Funtikov, T. Will (1994) Chloride adsorption on Ag(111) studied by in-situ scanning tunnelling microscopy, J. Electroanal. Chem., 370, 297-300. https://doi.org/10.1016/0022-0728(93)03140-K

[26] O. Magnussen, B.M. Ocko, R.R. Adžić, J.X. Wang (1995) X-ray diffraction studies of ordered chloride and bromide monolayers at the Au(111)-solution interface, Phys. Rev. B, 51, 5510-5518. https://doi.org/10.1103/PhysRevB.51.5510

[27] O. Magnussen, B.M. Ocko, J.X. Wang, R.R. Adžić (1996) In-Situ X-ray Diffraction and STM Studies of Bromide Adsorption on Au(111) Electrodes, J. Phys. Chem. B, 100, 5500-5508. https://doi.org/10.1021/jp953281j

[28] J.X. Wang, R.R. Adžić, B.M. Ocko, In Situ X-ray Scattering Studies of Electrosorption, in: A. Wieckowski (Ed.), Interfacial Electrochemistry: Accomplishments and Challenges, Marcel Dekker Inc., New York, 1999, pp. 175-185.

[29] Th. Wandlowski, J.X. Wang, B.M. Ocko (2001) Adsorption of bromide at the Ag(100) electrode surface, J. Electroanal. Chem., 500, 418-434. https://doi.org/10.1016/S0022-0728(00)00380-6

[30] O. Endo, D. Matsumura, K. Kohdate, M. Kiguchi, T. Yokoyama, T. Ohta (2000) In-situ XAFS studies of Br adsorption on the silver(111) electrode, J. Electroanal. Chem., 494, 121-126. https://doi.org/10.1016/S0022-0728(00)00338-7

[31] Z. Shi, J. Lipkowski (1996) Chloride adsorption at the Au(111) electrode surface, J. Electroanal. Chem., 403, 225-239. https://doi.org/10.1016/0022-0728(95)04313-6

[32] J. R. Macdonald, Impedance Spectroscopy Emphasizing Solid Materials and Systems, Wiley, New York, Chichester, Brisbane, Toronto, Singapore, 1987.

[33] T. P. Moffat, in: A. J. Bard and I. Rubinstein (Eds.), Electroanalytical Chemistry: aSeries of Advances, vol. 21, Marcel Dekker Inc., New York, Basel, 1999, pp. 211-316.

[34] G.J. Brug, A.L.G. Van Den Eedem, M. Sluyters-Rechbach, J.H. Sluyters (1984) The analysis of electrode impedances complicated by the presence of a constant phase element, J. Electroanal. Chem., 176, 275-295. https://doi.org/10.1016/S0022-0728(84)80324-1

[35] K.S. Cole, R.H. Cole (1941) Dispersion and Absorption in Dielectrics. I. Alternating Current Characteristics, J. Chem. Phys., 9, 341-351.

[36] J.-B. Jorcin, M.E. Orazem, N. Pébère, B. Tribollet (2006) CPE analysis by local electrochemical impedance spectroscopy, Electrochim. Acta, 51, 1473–1479 https://doi:10.1016/j.electacta.2005.02.128

[37] G. Láng, K.E. Heusler (2000) Comments on the ideal polarisability of electrodes displaying cpe-type capacitance dispersion, J. Electroanal. Chem., 481, 227–229 https://doi.org/10.1016/S0022-0728(99)00481-7

[38] G. Láng, K.E. Heusler (1998) Remarks on the energetics of interfaces exhibiting constant phase element behavior, J. Electroanal. Chem., 457, 257–260 https://doi.org/10.1016/S0022-0728(98)00301-5

[39] A.J. Motheo, A. Sadkowski, R.S. Neves (1997) Electrochemical immittance spectroscopy applied to the study of the single crystal gold/aqueous perchloric acid interface, J. Electroanal. Chem., 430, 253-262 https://doi.org/10.1016/S0022-0728(97)00255-6

[40] A. Sadkowski (2000) On the ideal polarisability of electrodes displaying cpe-type capacitance dispersion, J. Electroanal. Chem., 481, 222–226 https://doi.org/10.1016/S0022-0728(99)00480-5

[41] A. Sadkowski, (2000) Response to the 'Comments on the ideal polarisability of electrodes displaying cpe-type capacitance dispersion' by G. Láng, K.E. Heusler, J. Electroanal. Chem., 481, 232–236 https://doi.org/10.1016/S0022-0728(99)00483-0

[42] A. Sadkowski, A.J. Motheo, R.S. Neves (1998) Characterisation of Au(111) and Au(210) aqueous solution interfaces by electrochemical immittance spectroscopy[1], J. Electroanal. Chem.,455, 107–119 https://doi.org/10.1016/S0022-0728(98)00237-X

[43] P. Zoltowski (2000) Comments on the paper 'On the ideal polarisability of electrodes displaying cpe-type capacitance dispersion' by A. Sadkowski, J. Electroanal. Chem., 481, 230–231 https://doi.org/10.1016/S0022-0728(99)00482-9

[44] P. Zoltowski (1994)A new approach to measurement modelling in electrochemical impedance spectroscopy, J. Electroanal. Chem., 443, 45-57. https://doi.org/10.1016/0022-0728(94)13406-5

[45] C.H. Hsu, F. Mansfeld (2001) Technical Note: Concerning the Conversion of the Constant Phase Element Parameter Y0 into a Capacitance, Corr., 57, 747-748. doi:10.5006/1.3280607

[46] V.D. Jović (2003) Determination of the correct value of C_{dl} from the impedance results fitted by the commercially available software, Gamry Com./application-notes/EIS.

[47] V.D. Jović (2022) Calculation of a pure double layer capacitance from a constant phase element in the impedance measurements, Zastita Materijala, 63, 50-57. https://doi.org/10.5937/ZasMat2201050J

[48] V.D. Jović (2026) Adsorption of iodide anions onto Ag(111), Zastita Materijala, 67, 191-198. https://doi.org/10.62638/ZasMat1671

[49] J.N. Jovićević, V.D. Jović, A.R. Despić (1984) The influence of adsorbing substances on the lead UPD onto (111) oriented silver single crystal surface—I, Electrochim. Acta, 29, 1625-1638. https://doi.org/10.1016/0013-4686(84)89002-7

[50] K.J. Stevenson, X. Gao, D.W. Hatchett, H.S. White (1998)Voltammetric measurement of anion adsorption on Ag(111), J. Electroanal. Chem., 447, 43-51. https://doi.org/10.1016/S0022-0728(98)00021-7

[51] T. Yamada, K. Ogaki, S. Okubo, K. Itaya(1996) Continuous variation of iodine adlattices on Ag(111) electrodes: in situ STM and ex situ LEED studies, Surf. Sci., 369, 321-335. https://doi.org/10.1016/S0039-6028(96)00880-1

[52] J.H. Schott, H.S. White, (1994) Halogen adlayers on silver (111), J. Phys. Chem., 98, 291-297. https://doi.org/10.1021/j100052a049

[53] J.H. Schott, H.S. White (1994) Tunneling spectroscopy of halogen adlayers on silver (111) surfaces, J. Phys. Chem., 98 297-302. https://doi.org/10.1021/j100052a050

[54] J.H. Schott, H.S. White (1994) Halogen chemisorption on silver(111). Scanning tunneling microscopy of coadsorbed halogen atoms, Langmuir, 10, 486-491. https://doi.org/10.1021/la00014a024

[55] M. Kawasaki, H. Ishii (1995) Preparation and Surface Characterization of Ag(111) Film Covered with Halide Monolayer,Langmuir, 11, 832-841. https://doi.org/10.1021/la00003a026

IZVOD

ODREĐIVANJE KAPACITETA ADSORPCIJE I OTPORA ADSORPCIJE PRI ADSORPCIJI ANJONA

Ovaj revijalni rad sadrži rezultate ispitivanja adsorpcije anjona hlorida i bromida na monokristalima Ag(111), Ag(100) i na polikristalu Ag. Adsopcrija anjona ispitivana je primenom ciklične voltametrije (CV), elektrohemijske impedansne spektroskopije (EIS) i merenjem diferencijalnog kapaciteta (C_{diff}) u funkciji učestanosti (ω). Eksperimentalni rezultati impedanse su fitovani komercijalnim programom za fitovanje EIS 300(Gamry Instruments Inc.). Korišćeno je ekvivalentno kolo koje sadrži konstantni fazni element (CPE_{dl}) umesto kapaciteta dvojnog sloja (C_{dl}) u paralelnoj vezi sa kapacitetom adsorpcije (C_{ad}) i otporom adsorpcije (R_{ad}) (Slika 1(d)). Jednačina zavisnosti C_{diff}odω za ovakvo ekvivalentno kolo, definisana u prethodnim ispitivanjima, korišćena je za fitovanje eksperimentalno dobijenih C_{diff}vs.ω zavisnosti.

Pokazano je da se rezultati dobijeni fitovanjem impedanse pomoću komercijalnog programa i rezultati dobijeni fitovanjem C_{diff}vs.ω zavisnosti značajno razlikuju u svim ispitivanim sistemima, pri čemu su rezultati analize C_{diff}vs.ω zavisnosti pouzdaniji. Objašnjenje za razliku u rezultatima fitovanja je vrlo jednostavno. U slučaju upotrebe komercijalnog programa fituju se dve funkcije istovremeno, (Z'vs. ωi -Z'' vs. ω) dok se upotrebom zavisnosti C_{diff} vs.ω fituje samo jedna funkcija i normalno je očekivati da će rezultati fitovanja biti precizniji.

Ključne reči: *Ag monokristali, mehanizam adsorpcije anjona, EIS, CPE, zavisnost C_{diff}odω*

Pregledni rad
Rad primljen: 18.01.2026.
Rad prihvaćen: 25.02.2026.